

Statistical analysis of modification of joints of metals and composites by thermal drilling

Anna Guzanová^{1,*}, Nikita Veligotskyi¹, Gabriela Ižariková²
 Technical University of Košice, Faculty of Mechanical Engineering, Slovakia
 Department of Technology, Materials and Computer Supported Production¹
 Department of Applied Mathematics and Informatics²
 anna.guzanova@tuke.sk

Abstract: The paper presents an innovative method for joining Al alloy sheets and polymer fibre-reinforced composites by thermal drilling. A proposal for modifying the joint geometry by reverse drilling with a larger diameter tool is presented. The proposed modification demonstrated a statistically significant increase in the failure energy of the resulting joints.

Keywords: METAL-COMPOSITE JOINING, THERMAL DRILLING, BUSHING GEOMETRY, REVERSE DRILLING, STATISTICAL ANALYSIS, p-VALUE

1. Introduction

Thermal drilling represents a technique for joining dissimilar materials through the formation of bushings, even without fastener. In recent years, significant progress has been made in addressing the challenges associated with joining materials possessing fundamentally different physical and mechanical properties, such as thin-walled metallic and fiber reinforced composite substrates [1–7]. These hybrid material configurations are increasingly utilized in the design of ultralight structures, particularly within the automotive and aerospace sectors. Typical applications of metal–composite joints include structural elements such as A-pillars, engine covers, load-bearing plates, and front stretchers. Joints between thin-walled metal sheets and composite plates with a thermoplastic matrix are characterized by the preservation of fiber continuity, thereby maintaining their reinforcing function. To ensure this, the composite material must be heated above the melting temperature of the thermoplastic matrix during the joining process. Common thermoplastics used for the matrix include polypropylene, polyamide 6, polyamide 66, polyamide 12, polycarbonate, thermoplastic polyurethane, and polyphenylene sulfide. During the heating and formation of the metal bushing, the fibers within the composite are deflected, allowing the bushing to form without damage to the fibers.

The joint between the metal sheet and the composite, created through thermal drilling, may appear as shown in Fig. 1.



Fig. 1 Schematic representation of a possible joint failure

As seen in Fig. 1, the joint is mechanical; however, due to the heating of the polymer matrix and the mutual compression of the materials during the joining process, adhesive bonding also occurs between the materials. The end of the bushing is used for hemming flange the joint, which prevents it from opening under stress. The outer surface of the bushing is conical, while the inner surface is cylindrical. Fig. 1 also highlights the potential modes of failure of the joint under tensile loading. In an ideal case, the joint should fail by shear of the bushing, but practical experience has shown that due to the conical shape of the bushing, failure occurs more often by the composite slipping off the conical bushing, straightening of the hem, or shearing of the hem, leading to the composite being pulled out of the bushing. As a result, the materials separate without fully utilizing the material properties of the metal (bushing), and the joint fails.

The aim of this paper is to present the proposed change in the geometry of the bushing and its effect on the effective use of the material properties of the metal parts of the joint.

2. Materials and methods

The metal sheet used for the joint formation is made of EN AW 6082 T6 alloy with a thickness of 1 mm. This is a precipitation-hardened aluminum alloy, commonly used in the manufacturing of lightweight structures in the automotive industry or construction.

For the composite, polypropylene with a melting temperature of 165°C, reinforced with glass fibers (GF) and carbon fibers (CF), was used. The fibers are continuous and laid in two mutually perpendicular directions in the form of a mat. The thickness of the composite panels was 1.5 mm, with the thickness of the glass fiber panels achieved by consolidating three layers of prepreg, while the carbon fiber panels consisted of seven layers.

The joint was created by thermal drilling using a Flowdrill Long tool $\varnothing 5.3$ mm, with the following process parameters: RPM 4800 min^{-1} , feed rate 60 $\text{mm} \cdot \text{min}^{-1}$. During drilling, the materials (Al-CF, Al-GF) were overlapped on a length of 30 mm, and the composite was heated to 175°C, as shown in Fig. 2. Forty joints were produced for each material combination to allow for a detailed statistical analysis of the results.

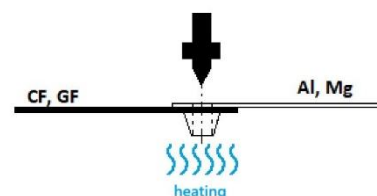
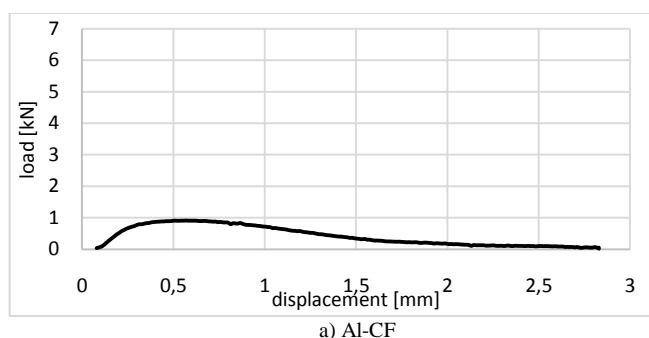


Fig. 2 Principle of joint formation by thermal drilling

Load-displacement dependence was recorded when testing the load-carrying capacity of the connections.

Results

Selected load-displacement curves for Al-CF and Al-GF joints are shown in Fig. 3.



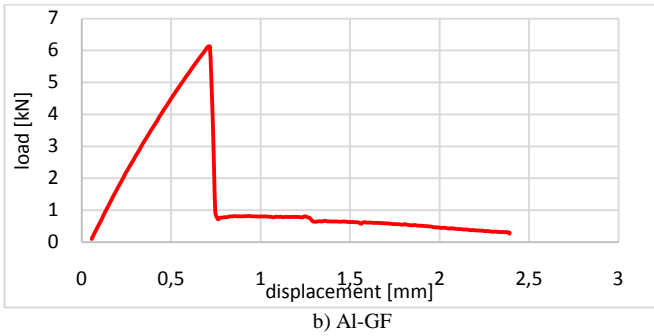
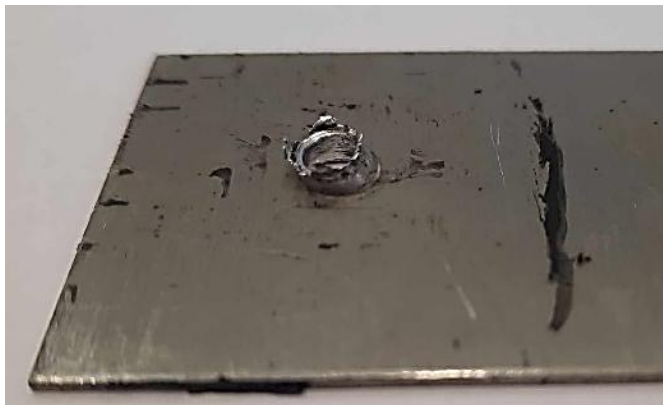


Fig. 3 Load-displacement curves when testing load-bearing capacity of joints

In Al-CF joint, there was no adhesive bonding, only mechanical joining through the bushing. In the case of Al-GF joints, the curve first shows an increase in force up to F_{max} , when the adhesive part of the joint was broken and the force dropped sharply. At this point, the load was transferred to the joint bushing which deformed and the composite was gradually pulled out of the joint, Fig. 4.



a) bushing deformation, straightening of the hem

b) hem shear

Fig. 4 Mechanism of bushing failure in joints

To prevent the composite from sliding out of the bushing, a geometric modification of the bushing was proposed by forming an inverted cone with a tool of larger diameter (9.3 mm) than the original bore (5.3 mm), which would eliminate the tangential component of the force that leads to the composite sliding out of the bushing, Fig. 5. The process of modifying the geometry of the bushing will be referred to as reverse drilling (RD) in this context.

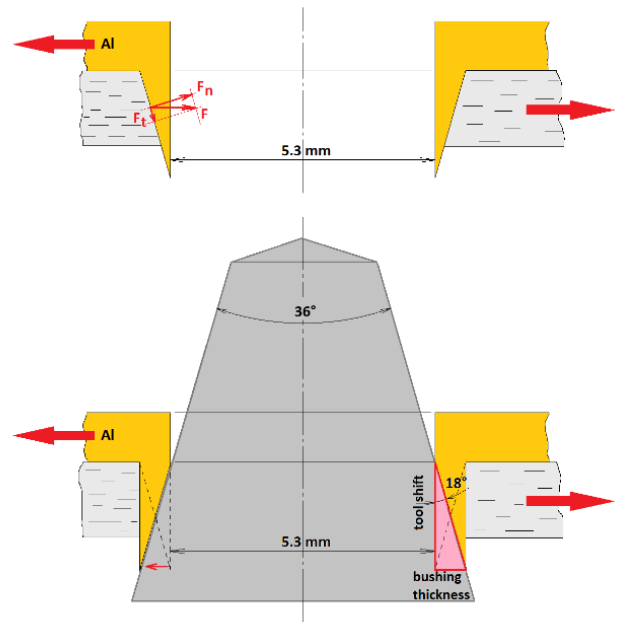
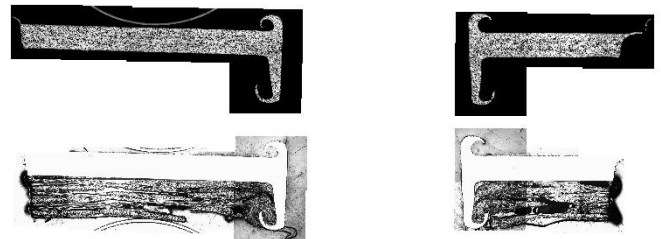
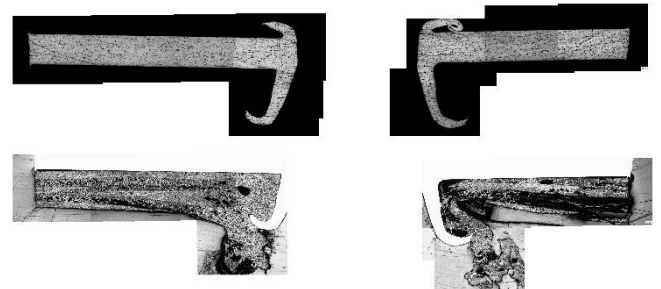


Fig. 5 Design of the bushing geometry modification to increase the load carrying capacity of the connections (F - loading force, F_n - normal, F_t - tangential component of the force F)

In reverse drilling the shape of the bushing changes to the opposite - the outer shape is cylindrical, the inner conical, Fig. 5 and 6.



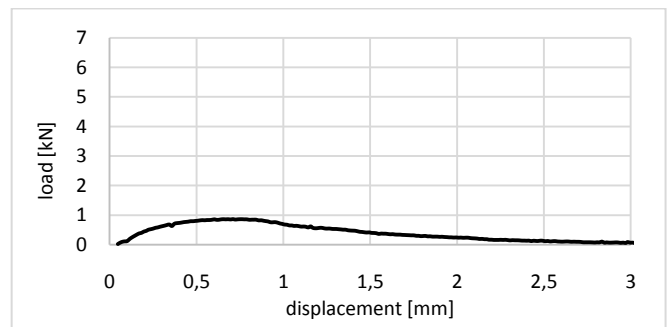
a) Al-GF, thermal drilling and hemming flange



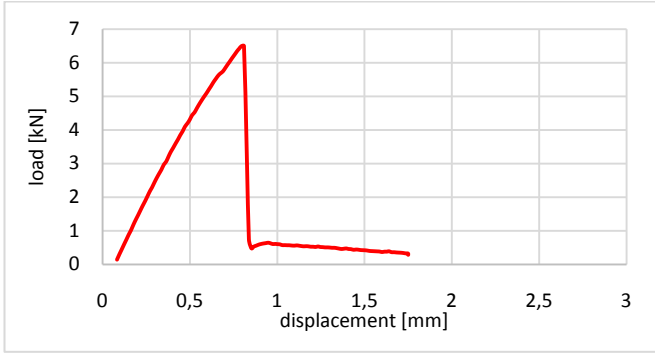
b) Al-GF, thermal drilling, hemming flange, RD

Fig. 6 Metallographic section of Al-GF joint

The joints, modified by reverse drilling (RD) were also stressed in tension, Fig. 7.



a) Al-CF RD



b) Al-GF RD

Fig. 7 Load-displacement curves when testing load-bearing capacity of joints with improved bushing geometry by reverse drilling

At first glance, the load-displacement curves appear very similar, which is why it was necessary to analyze the resulting dependencies in more detail using statistical methods. The load-displacement relationships also serve as the basis for calculating another indicator, beyond just the maximum force F_{max} , namely the energy W dissipated at the failure of the joint. It is desirable for the joint to absorb as much energy W (in joules) as possible during failure, thereby contributing to the overall impact absorption during a vehicle collision in the vehicle's deformation zones and joints. The dissipated energy is calculated using the following formula:

$$W = \int_0^{s_{max}} F(s)ds \approx \sum_{i=1}^n F_i(\bar{s}_i)\Delta s = \Delta s[F_1(\bar{s}_1) + F_2(\bar{s}_2) + \dots + F_n(\bar{s}_n)]$$

where F_i is the instantaneous value of the load in N and s_i is the instantaneous value of the displacement in m .

Additionally, it can be seen that the load-displacement curve can be divided into two parts – the adhesive and mechanical part of joint, Fig. 8, and the dissipated energy for both components of the joint can be calculated separately, as shown in Table 1.

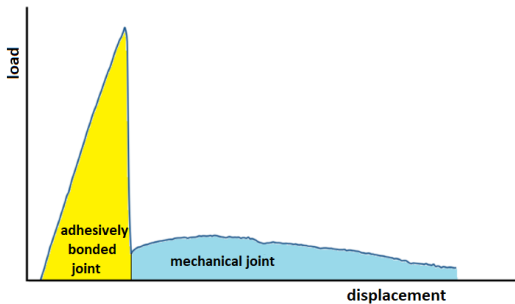


Fig. 8 Typical load-displacement curve for a hybrid, adhesion-mechanical joint

Tab. 1 Energy dissipated in the particular areas of the hybrid joints

Joint	Adhesive part		Mechanical part		Total energy		Change in energy [%]
	[J]	[%]	[J]	[%]	[J]	[%]	
Al-CF	0.00	0.00	1.07	100.00	1.07	100.00	+37.33
Al-CF RD	0.00	0.00	1.47	100.00	1.47	100.00	
Al-GF	1.81	79.23	0.48	20.77	2.29	100.00	+27.96
Al-GF RD	2.13	71.66	0.80	28.34	2.93	100.00	

As seen in Table 34, modifying the bushing geometry resulted in an increase in the total energy consumed during failure for all joint types, as well as an increase in the partial energies in the adhesive and mechanical parts of the joint. The failure mode of the joint also changed, from bushing deformation to bushing shear (Fig. 9), which is desirable for the efficient utilization of the material properties of the aluminum alloy.



a) Al-GF RD, partial shear of the bushing (approx. 1/3 of the circumference), the bushing remains part of the Al plate



b) Al-CF RD, partial shear of the bushing (approx. 2/3 of the circumference), the bushing remains wedged in the CF



c) Al-CF RD, total shear of the bushing, the bushing remains wedged in the CF

Fig. 9 Mechanism of bushing failure in Al-composite hybrid joints with bushing geometry modification by reverse drilling

The percentage representation of the failure modes of the joints before and after the geometry modification through reverse drilling, based on testing 40 joints in each group, is shown in Fig. 10.

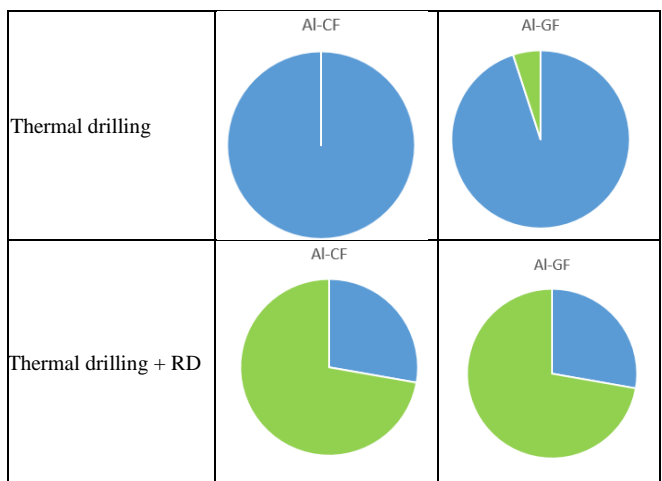


Fig. 10 Change in the joint failure mode (blue - deformation of the bushing, pulling out of the composite, green - shearing of the bushing)

By modifying the bushing geometry, the proportion of joints failed by bushing shear significantly increased, which was the objective of the proposed bushing modification.

To compare the data sets (maximum force F_{max} , energy W consumed during joint failure), statistical tests were used. The normality condition was verified using the Shapiro-Wilk test (SW) to determine whether it is appropriate to use a parametric or non-parametric test. The Shapiro-Wilk normality test evaluates the validity of the following hypotheses:

H_0 : the data set has a normal distribution

H_1 : the data set does not have a normal distribution

Subsequently, Fisher's F-test was used to test the hypothesis regarding the equality of variances of two independent data sets. The hypotheses tested were:

H_0 : the two independent data sets have equal variance

H_1 : the two independent data sets do not have equal variance

Based on the results of the F-test, the Student's t-test for two independent samples was used for the comparison, either assuming equal variances or unequal variances. This test evaluates the hypothesis about the difference in the means of two data groups and is used to determine whether the observed difference in means from the samples is due to chance or is statistically significant.

Tested hypotheses:

H_0 : the difference in the means of two independent data sets is not statistically significant

H_1 : the difference in the means of two independent data sets is statistically significant

There are various ways to test the hypotheses H_0 against H_1 at the significance level α (in our case $\alpha=0.05$), and although these methods may differ, the conclusion remains the same. The acceptance or rejection of the null hypothesis is based on the p-value as follows:

- if $p < \alpha$, the null hypothesis H_0 is rejected at the significance level α in favor of the alternative hypothesis H_1 ,
- if $p > \alpha$, the null hypothesis H_0 cannot be rejected.

The statistical tests mentioned above were used to compare the different categories of joints created by thermal drilling and reverse drilling with modified bushing geometry, both in terms of the achieved maximum force F_{max} during joint load testing and in terms of the energy W dissipated during joint failure, as shown in Tab. 2 and 3.

Tab. 2 Statistical comparison of Al-composite joints in terms of F_{max}

Joints	Al-CF	Al-CF RD	Al-GF	Al-GF RD
SW test				
p-value	0.2815	0.1619	0.2530	0.0547
conclusion	$p > \alpha$ normal distribution, parametric tests	$p > \alpha$ normal distribution, parametric tests	$p > \alpha$ normal distribution, parametric tests	$p > \alpha$ normal distribution, parametric tests
F-test				
p-value	0.000621184		0.041717792	
conclusion	$p < \alpha$ data sets do not have equal variance, unequal variances T-test		$p < \alpha$ data sets do not have equal variance, unequal variances T-test	
t-test				
p-value	0.062563566		0.074745448	
conclusion	$p > \alpha$ The difference in means is not statistically significant		$p > \alpha$ The difference in means is not statistically significant	

Tab. 3 Statistical comparison of Al-composite joints in terms of W

Joints	Al-CF	Al-CF RD	Al-GF	Al-GF RD
SW test				
p-value	0.8878	0.548	0.9638	0.9547
conclusion	$p > \alpha$ normal	$p > \alpha$ normal	$p > \alpha$ normal	$p > \alpha$ normal

	distribution, parametric tests	distribution, parametric tests	distribution, parametric tests	distribution, parametric tests
F-test				
p-value	0.0592		0.5301	
conclusion	$p > \alpha$ data sets have equal variance, equal variance T-Test		$p > \alpha$ data sets have equal variance, equal variance T-Test	
t-test				
p-value	0.0000		0.000373	
conclusion	$p < \alpha$ The difference in means is statistically significant		$p < \alpha$ The difference in means is statistically significant	

The statistical tests confirmed that, although the maximum force at joint failure F_{max} does not change statistically significantly with the modification of the bushing geometry, the increase in the total energy W dissipated during the failure of joints with modified bushing geometry—across all tested material combinations—is not random, but statistically significant at the 0.05 significance level.

Conclusion

Experimental and statistical tools have confirmed that by modifying the tool geometry through reverse drilling with a larger diameter tool, it is possible to achieve a more efficient utilization of the mechanical properties of metallic parts when joining metals and composites using the thermal drilling technology.

Acknowledgement: This work was supported by The Ministry of Education, Research, Development and Youth of the Slovak Republic under Grant VEGA 1/0229/23: Research on the applicability of thermal drilling technology for the creation of multi-material joints in the automotive industry.

References

- [1]. XIN, Z. – LIU, L. – CHEN, T. – WU, L. – CHEN, K. – KONG, L. – WANG, M.: Laser surface treatment to enhance the adhesive bonding between steel and CFRP: Effect of laser spot overlapping and pulse fluence. In: Optics & Laser Technology 22, 59 (2023), 1-12, 10.1016/j.optlastec.2022.109002.
- [2]. LAMBIASE, F. – KO, D.: Two-steps clinching of aluminum and Carbon Fiber Reinforced Polymer sheets. In: Composite Structures 17, 164 (2017), 180-188, <https://doi.org/10.1016/j.compstruct.2016.12.072>.
- [3]. GUZANOVÁ, A. – JANOŠKO, E. – VELIGOTSKYI, N.: Optimization of joining parameters of thin-walled materials by flowdrill technology. In: MACHINES. TECHNOLOGIES. MATERIALS 22, 5 (2022), 176-178, ISSN 1313-0226.
- [4]. GUZANOVÁ, A. – JANOŠKO, E.: Application of flow-drill technology for joining metal materials. In: INNOVATIONS 21, 3 (2021), 108-111, ISSN 2603-3763.
- [5]. SEIDLITZ, H. – ULKE-WINTER, L. – KROLL, L.: New Joining Technology for Optimized Metal/Composite Assemblies. In: Journal of Engineering 14, 1-11, <http://dx.doi.org/10.1155/2014/958501>.
- [6]. TROSCHITZ, J. - FÜBEL, R. – KUPFER, R. – GUDE, M.: Damage Analysis of Thermoplastic Composites with Embedded Metal Inserts Using In Situ Computed Tomography. In: Journal of Composites Science 22, 6 (2022), 1-9, <https://doi.org/10.3390/jcs6100287>.
- [7]. GROGER, B. et al.: Computed tomography investigation of the material structure in clinch joints in aluminium fibre-reinforced thermoplastic sheets. In: Production Engineering 22, 16 (2022), 203-212, <https://doi.org/10.1007/s11740-021-01091-x>.